Advanced lab course for Bachelor's students

Versuch T2

Gamma spectroscopy and Compton scattering

February 2018

Prerequisites

- Interactions of photons and matter
- Working principle and usage of scintillation counters

Experimental goal

- Energy spectroscopy of different sources of γ-radiation
- Measurement of Compton scattering
- Measurement of the differential scattering cross-section
- Measurement of the electron mass

Contents

References

[1] Brian Williams: Compton Scattering, Bo 145

[2] William R. Leo: Techniques for Nuclear and Particle Physics Experiments, Dr 155
(Kapitel 2.7, Kapitel 7, Kapitel 8)

[3] Konrad Kleinknecht: Detektoren f"ur Teilchenstrahlung, Dr 143

[4] Peter Schm"user: Feynman-Graphen und Eichtheorien f"ur Experimentalphysiker, Bs 301

[5] National Institute of Standards and Technology: Physical Reference Data
`http://physics.nist.gov/PhysRefData/XrayMassCoef/cover.html`

1 Energy spectroscopy of γ-radiation

1.1 Interactions of photons and matter

When photons encounter matter, they can interact with the shell electrons or with the atomic nuclei through different processes. In this lab course, γ-radiation in the energy range from 5 keV up to 2 MeV are used. In this range, for the purpose of this lab course, it is sufficient to take into account the interactions with the highest probability of occurrence, that are:

- **Photoelectric effect:** The photoelectric effect takes place when a photon with energy E_γ is absorbed by a shell electron with binding energy E_B, and $E_\gamma > E_B$. The photon transmits all its energy to the electron, allowing the electron to be released from its bound state with a kinetic energy that is $E_{\text{kin}} = E_\gamma - E_B$.

  Using the Born approximation to calculate the interaction cross-section yields

  $$\sigma_{\text{Photo}} \propto \begin{cases} \frac{Z^5}{E_\gamma^{7/2}} & E_\gamma \ll m_\text{e} c^2 \\ \frac{Z^5}{E_\gamma} & E_\gamma \gg m_\text{e} c^2 \end{cases}$$

  Where Z is the charge number of the nucleus and m_e is the electron rest mass.

- **Compton scattering:** Photons with larger energies may be deflected by shell electrons. Compton scattering is dominant over the photoelectric effect when E_γ is sufficiently large for the binding energy to be negligible. The electron may then be considered effectively free. In contrast to the case of photoelectric effect, the photon is not absorbed in case of Compton scattering, but transfers energy to the electron. The scattering cross-section is calculated as

  $$\sigma_{\text{Compton}} \propto Z \cdot f(E_\gamma),$$

  where $f(E_\gamma)$ is a decreasing function.

- **Pair production:** If the energy of the photon is larger than two times the electron rest mass, an electron-positron pair may be created from the photon. Since energy and momentum must be conserved in this reaction, it is only possible if an additional body (such as an atomic nucleus) participates. Therefore, the threshold energy is not exactly $2m_\text{e}c^2$ but

  $$E_\gamma^{\text{min}} = 2m_\text{e}c^2 \left(1 + \frac{m_\text{e}}{M}\right).$$

  where M is the mass of the interaction partner. The total cross-section is

  $$\sigma_{\text{Pair}} \propto Z^2 \ln E_\gamma.$$

The mass absorption coefficient or mass attenuation coefficient, that characterizes how easily the material can be penetrated by the radiation, is given by $\mu' = \mu/\rho$ (where μ is the attenuation coefficient of the material and ρ is the density) and it is proportional to the cross-section σ. It is shown in Figure 1 for the absorption of γ-rays in lead.

1.2 Measurement of the energy spectrum

The procedure for measuring an energy spectrum is schematically shown in Figure 2. Incoming photons deposit energy in the scintillator material due to ionization, producing radioluminiscence light flashes that are propagated to the photo cathode of the photo multiplier. In the photo multiplier, electrons are released and their numbers are enhanced due to an avalanche release of further electrons. The electron signal is amplified and its shape is manipulated before being fed into a multi channel analyser (MCA). The MCA sorts the incoming pulses by height and creates a pulse height diagram.

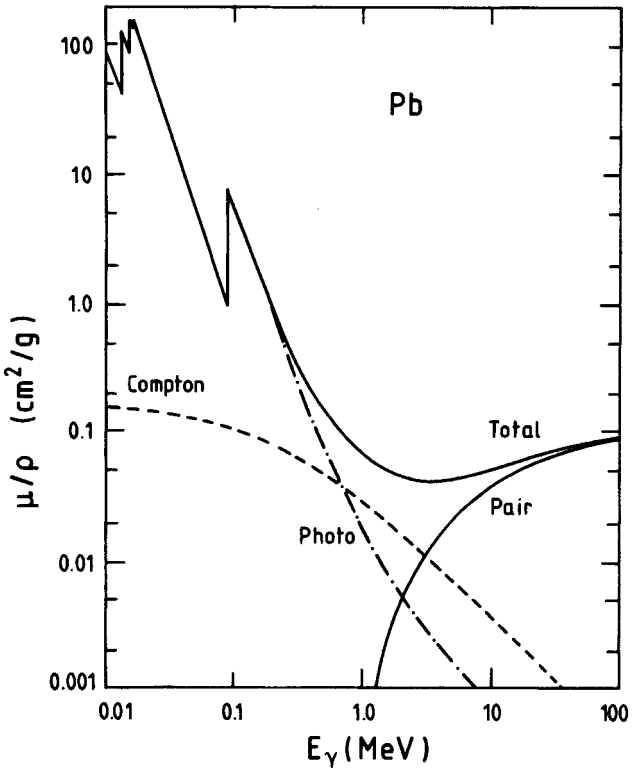

Figure 1: Mass absorption coefficient for photoelectric effect, Compton effect and pair production in lead as a function of the energy of the incoming photon. [3]

Photo spectrum

In the photoelectric effect, an electron is removed from an inner shell of an atom acquiring an energy of $E_\mathrm{e} = E_\gamma - E_B$, where the second term represents the electron binding energy. For NaI(Tl), when an electron is removed from the K shell of an iodine atom (binding energy $E_B = 36\,\mathrm{keV}$). The unoccupied state left behind by the electron is filled by an electron from one of the higher shells, leading to the emission of x-ray photons, which may again be absorbed via photoelectric effect. Absorption of these secondary photons in the scintillator causes an additional peak with energy E_γ. X-ray photons that leave the scintillator material cause a peak with energy $E_\mathrm{e} = E_\gamma - E_B$. Because of the limited resolution of the detector, not two sharp lines, but rather a Gaussian distribution is observed. The theoretical and experimental spectra of the photoelectric effect are shown in Figure 3.

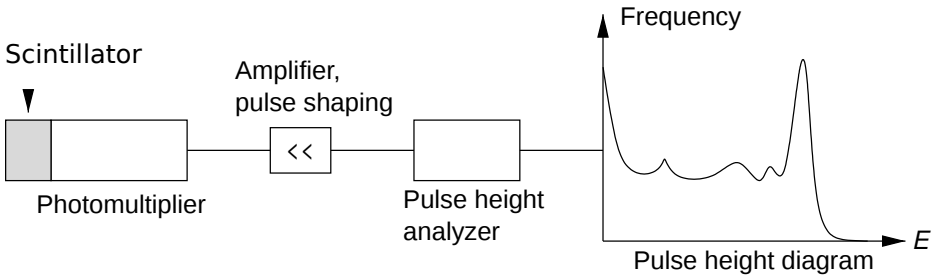

Figure 2: Measurement of a pulse height diagram.

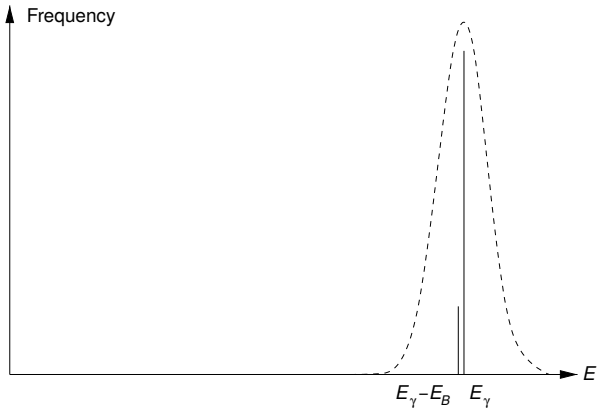

Figure 3: Pulse height diagram of the photoelectric effect. Theoretical (solid lines) and experimentally observed (dashed line) curves are shown.

Compton scattering

For $E_\gamma > 200\,\mathrm{keV}$ the Compton effect begins to dominate the photonic behavior in the NaI(Tl) crystal. The electrons released via the Compton effect do not receive the complete energy E_γ but have a continuous energy spectrum. The energy of the electron is maximal for a central collision between photon and electron ($\theta = 180°$). In this case the energy is (see eq. 4):

$$E_\mathrm{e}^\mathrm{max} = E_C = \frac{E_\gamma}{1 + \dfrac{m_\mathrm{e}c^2}{2E_\gamma}}$$

This maximal energy is also called Compton edge E_C. E_e is reduced for non-central collisions (see Figure 4). The theoretical cross section depending on the energy and scattered angle is described by the Klein-Nishina formula (see eq. 3)). The experimentally observed curve (Figure 4) is smeared out by the limited detector resolution.

Simulations that use a gaussian resolution curve show that the theoretical maximal energy E_C rather accurately corresponds to the experimental energy at which the falling flank crosses 70 % of the height of the maximum. For most regions, this result does not depend on the width of the resolution curve.

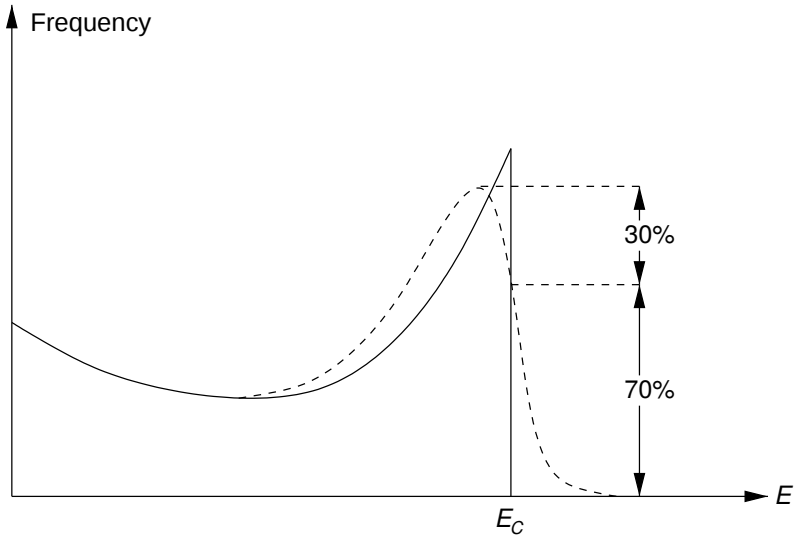

Figure 4: Distribution of Compton energies of electrons. Theoretical Klein-Nishina (solid line) and experimental (dashed line) curves are shown.

Combined theoretical and experimental spectra of photoelectric and Compton effect are shown in Figure 5. In addition to photo peak, photo-escape peak, Compton edge and a continuous component, the spectrum also contains the backscatter peak at E_R. This peak is the result of Compton scattering that occurs anywhere other than in the scintillator material. Photons scattered in the surrounding parts of the detector setup may enter the detector and deposit their reduced energy E'_γ. The energy distribution of the scattered photons is equal to the energy distribution of the Compton electrons with inverted x-axis (Figure 4). Its maximum is given by $E_R = E'_\gamma = E_\gamma - E_C$.

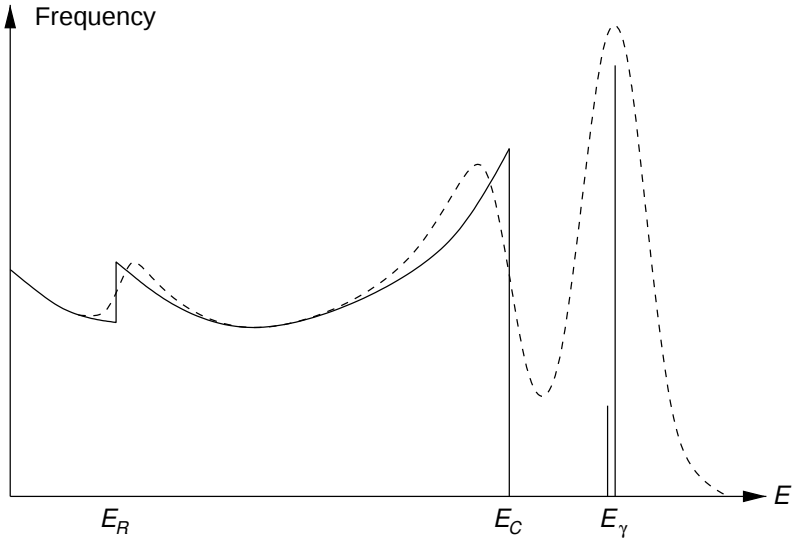

Figure 5: Combined pulse height diagram of photo and Compton effects. Theoretical (solid line) and experimental (dashed line) curves are shown.

Pair production spectrum

For the case of pair production, the electron-positron pair is decelerated and it forms a bound e^+e^-, the so called positronium. The positronium state is unstable and it decays into either two photons (Parapositronium: the spin directions are anti-parallel) or three photons (Orthopositronium: the spin directions are parallel). Assuming that the positronium state is at rest, conservation of energy and momentum dictates that the photons produced in a parapositronium decay are emitted back to back with an energy of $E_\gamma = m_e c^2$ each. Since one or both of the photons may leave the scintillator undetected, additional peaks are observed at energies reduced by $m_e c^2 = 511\,\mathrm{keV}$ per undetected photon.

Combined spectrum of all processes

Figure 6 shows the measured spectrum of photons with an initial energy of $E_\gamma = 2\,\mathrm{MeV}$, recorded using a NaI(Tl) scintillation counter. The spectrum contains structures resulting from multiple processes:

- $E_\gamma = 2{,}00\,\mathrm{MeV}$: Photo peak, absorption of the complete energy E_γ by
  - Photoelectric effect
  - Compton effect with absorption of the scattered photon
  - Pair production with absorption of both final state photons.
- $E_C = 1{,}77\,\mathrm{MeV}$: Compton edge caused by the Compton effect in central collisions where the scattered photon is lost.
-
- $E^{(1)}_{\mathrm{esc}} = E_\gamma - m_e c^2 = 1{,}49\,\mathrm{MeV}$: Escape peak caused by pair production, where one of the final state photons escaped undetected.

- $E_{\text{esc}}^{(2)} = E_\gamma - 2m_e c^2 = 0{,}98\,\text{MeV}$: Double escape peak caused by pair production, where both of the final state photons escaped undetected.
- $E_R = E_\gamma - E_C = 0{,}23\,\text{MeV}$: Backscatter peak caused by the Compton effect outside of the scintillator, where the scattered photon is absorbed in the scintillator.

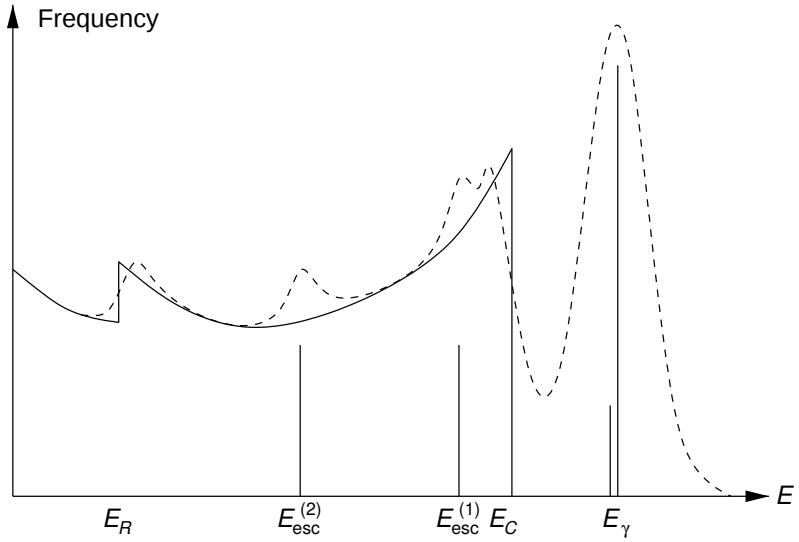

Figure 6: Spectrum of photons with an initial energy of 2 MeV

1.3 Resolution

We do not observe sharp lines where we expect to see them in the spectrum, but rather a Gaussian distribution is observed due to the limited resolution of the detector (see Figure 3). The energy resolution is given by

$$\frac{\Delta E}{E} = a \oplus \frac{b}{\sqrt{E}} = \sqrt{a^2 + \frac{b^2}{E}} \tag{1}$$

Where E is the energy of the incident particles. The second term $b/\sqrt{E}$ is the result of Poisson statistics, which governs the creation of scintillation photons. The first term a represents all other processes that influence the energy resolution.

2 Compton scattering

Scattering of photons with electrons is called Compton scattering:

$$\gamma + \mathrm{e} \to \gamma + \mathrm{e}$$

Consider an incoming photon with energy E_γ, which is scattered off an electron at rest by an angle θ. The energy E'_γ of the scattered photon is then

$$E'_\gamma = E_\gamma \cdot \frac{1}{1 + a(1 - \cos\theta)} \quad \text{where} \quad a = \frac{E_\gamma}{m_\mathrm{e} c^2}$$

The electron receives the kinetic energy E_e, which is maximal for a central collision:

$$E_\mathrm{e} = E_\gamma - E'_\gamma = E_\gamma \cdot \frac{a(1 - \cos\theta)}{1 + a(1 - \cos\theta)} \quad \overset{\theta=180^\circ}{\longrightarrow} \quad E_\mathrm{e}^{\max} = E_\gamma \cdot \frac{2a}{1 + 2a} \tag{2}$$

The energy distributions as a function of the scattering angle are shown in Figure 7

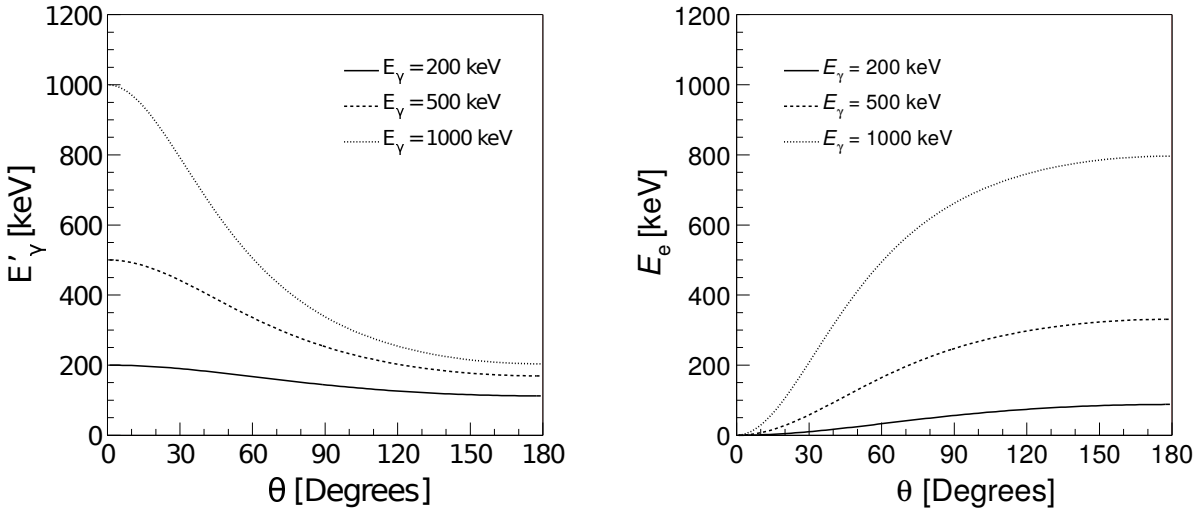

Figure 7: The energy distributions of scattered photons (E'_γ) and electrons (E_e) as a function of the scattering angle θ.

The differential interaction cross-section is given by the Klein-Nishina formula [4]:

$$\frac{d\sigma}{d\Omega} = \frac{\alpha^2 \lambda_\mathrm{e}^2}{8\pi^2} \cdot \frac{1}{\rho^2} \left(\rho + \frac{1}{\rho} - \sin^2\theta \right) \quad \text{where} \quad \rho = \frac{E_\gamma}{E'_\gamma} = 1 + a(1 - \cos\theta) \tag{3}$$

The so called Compton wavelength of the electron λ_e is defined by

$$\lambda_\mathrm{e} = \frac{h}{m_\mathrm{e} c} = 2{,}4 \cdot 10^{-12}\,\mathrm{m}.$$

By integrating over all scattering angles, we obtain the total cross-section:

$$\begin{aligned}
\sigma_\mathrm{tot} &= \int \frac{d\sigma}{d\Omega}\, d\Omega \\
&= \frac{\alpha^2 \lambda_\mathrm{e}^2}{8\pi^2} \int_0^{2\pi} \int_0^{\pi} \frac{1}{\rho^2} \left(\rho + \frac{1}{\rho} - \sin^2\theta \right) \sin\theta \, d\theta \, d\phi \\
&= \frac{2\pi\alpha^2 \lambda_\mathrm{e}^2}{4\pi^2 a^2} \left(\frac{2 + a(1+a)(8+a)}{(1+2a)^2} + \frac{(a-1)^2 - 3}{2a} \cdot \ln(1+2a) \right)
\end{aligned}$$

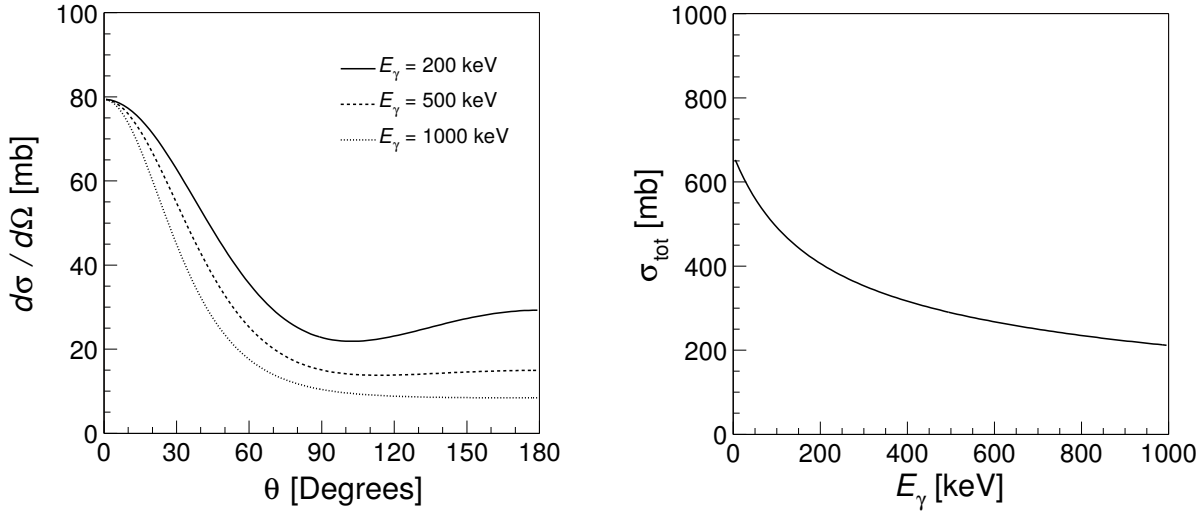

Figure 8: Differential and total interaction cross-section of Compton scattering.

Differential and total cross-section of Compton scattering are shown in Figure 8.

In scintillation spectroscopy, the observed instance of Compton scattering commonly occurs in the scintillating material. If the scattered photon leaves the scintillator undetected, only the scattered electron contributes to the scintillator pulse height. Using $a = E_\gamma / m_\mathrm{e}c^2$ and $b = E_\mathrm{e}/m_\mathrm{e}c^2$ we obtain the pulse height spectrum that reflects the energy distribution of the Compton electrons. Using $dE_\mathrm{e}/d\cos\theta$ in eq. 2 to transition from $d\sigma/d\Omega$ to $d\sigma/dE_\mathrm{e}$ yields:

$$\frac{d\sigma}{dE_\mathrm{e}} = \frac{\alpha^2\lambda_\mathrm{e}^2}{16\pi^3 m_\mathrm{e}c^2} \cdot \frac{1}{a^2}\left(\frac{b^2}{a^2(a-b)^2} + \frac{(b-1)^2-1}{a(a-b)} + 2\right) \tag{4}$$

This spectrum has a sharp edge at $E_\mathrm{e}^\mathrm{max}$ (see Figure 4), the so called Compton edge (E_C).

2.1 Cross-section measurement

The differential cross-section $d\sigma/d\Omega$ is defined as the ratio between the counting rate dm in the solid angle element $d\Omega$ to the flux Φ of incoming particles:

$$\frac{d\sigma}{d\Omega} = \frac{1}{\Phi}\frac{dm}{d\Omega}$$

For the counting rate of a detector that covers a solid angle $\Delta\Omega$ we obtain:

$$m = \frac{A \cdot I_\gamma}{4\pi r_0^2} \int\limits_{\Delta\Omega} \frac{d\sigma}{d\Omega}\, d\Omega \qquad \text{(For a single scattering body)} \tag{5}$$

Photons emitted by a source with activity A and photon yield I_γ encounter a scattering body at distance r_0 (Figure 9). The particles are scattered under an angle θ and are detected in a sensitive volume that covers the solid angle $\Delta\Omega$. The Detector is located at a distance r from the scattering body and is insulated with lead blocks from the initial radiation.

Using (5) we obtain for the count rate:

$$m = \frac{A \cdot I_\gamma}{4\pi r_0^2} \cdot \eta \cdot \varepsilon \cdot N_\mathrm{e} \cdot \frac{d\sigma}{d\Omega} \cdot \frac{F_D}{r^2} \tag{6}$$

Where

A = Source activity

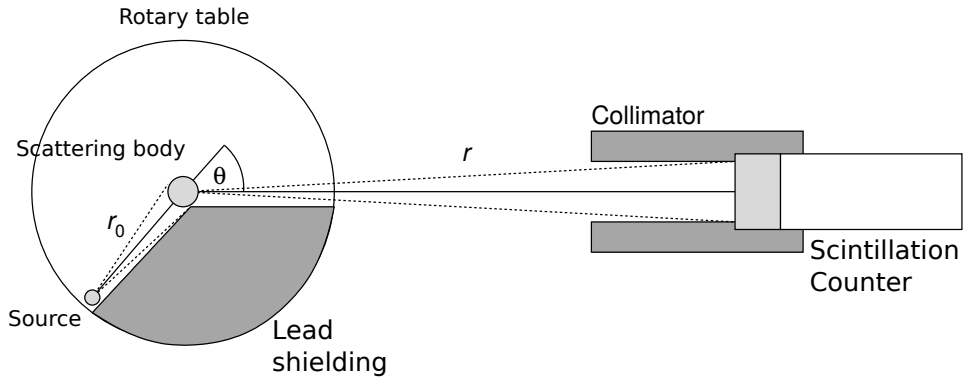

Figure 9: Conventional geometry for the large angle measurement.

I_γ	=	Source photon yield
r_0	=	Distance of scattering body and source
$\frac{A}{4\pi r_0^2}$	=	Particle flux at the location of the scattering body
η	=	Absorption in air and scattering body
ε	=	Detector efficiency
N_e	=	Number of electrons in the scattering volume
$\frac{d\sigma}{d\Omega}(\theta, E_\gamma)$	=	Differential scattering cross-section
F_D	=	Sensitive area of the detector
r	=	Distance of detector and scattering body
$\frac{F_D}{r^2}$	=	Solid angle $\Delta\Omega$ covered by the detector

To measure Compton scattering at large angles, the so called conventional geometry (Figure 9 is used. The source is located on a rotary table, which allows different angles to be probed. Lead blocks insulate the scintillator from initial radiation. However, the conventional geometry does not allow measurements at small scattering angles. In this case, photons scattered in collimators and the lead shielding would dominate the measured spectrum. Therefore, the so called ring geometry is used for measurements at small angles (Figure 10).

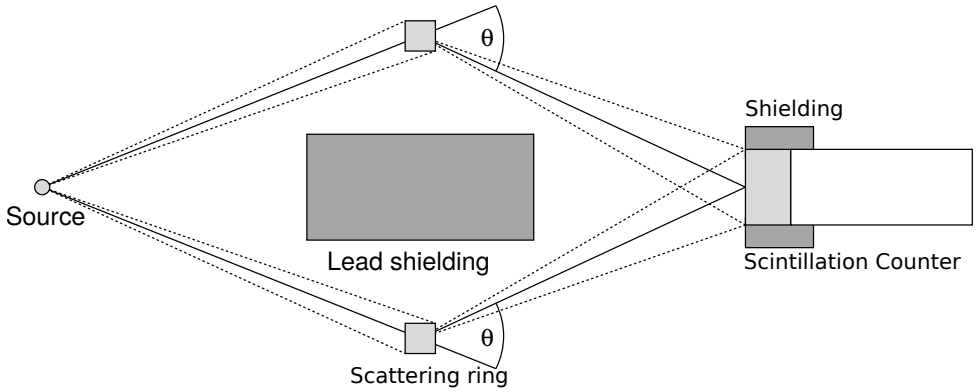

Figure 10: Ring geometry for the measurement of scattering at small angles.

The setup is axially symmetric to the connecting line between source and detector. A sufficiently long absorbing cylinder is placed on the connecting line to shield the detector from initial photons. A ring

around the symmetry axis is used as scattering body. The scattering angle may be adjusted via the distances between source, scattering body and detector. The advantages of this geometry are:

- large scattering volume and good angular resolution
- measurement at small angles
- good shielding of initial photons

Disadvantages include:

- not suited for measurements at large angles
- additional background caused by scattering in the environment of the experimental setup

The count rate m is still given by eq. 6.

2.2 Detection efficiency

The detection probability (efficiency) of a detector is defined by $\varepsilon = m/m_0$ where m_0 is the rate of incoming particles and m the rate of counted pulses (count rate).

The efficiency depends on the kind and size of sensitive volume as well as the kind and energy of incoming radiation. A further factor may be the electronic implementation of the detector. When using a single kind of detector, the energy dependence of the detection efficiency is especially important.

In this experiment the efficiency of a NaI(Tl) scintillation counter is needed for γ radiation of different energies. The simplest way of determining ε is by using mono-energetic sources with known activity A and photon yield I_γ at a defined distance r from the detector. The efficiency may then be calculated from a measurement of the count rate

$$m = \frac{A \cdot I_\gamma}{4\pi r^2} \cdot F_D \cdot \varepsilon$$

(Figure 11).

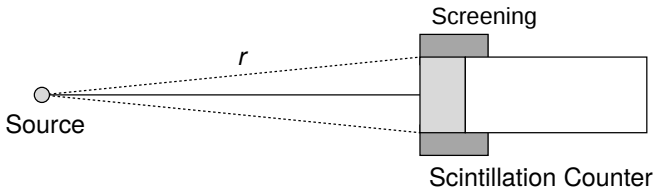

Figure 11: Efficiency measurement using direct radiation.

The mono-energetic photons create a pulse height spectrum in the scintillator. Therefore, the measured efficiency depends on the range of the pulse height spectrum used for the measurement. A sensible choice is the region of the photo peak.

3 Execution

3.1 Setup

All settings (voltage for the photomultiplier **max. 700 V**) are set using software since scintillator, photomultiplier, high voltage source and multi-channel analyser (MCA) are connected and evaluated via USB. The "stabiliser option" should be switched off. In the execution, the settings should stay constant and they should be controlled in the measurement.

3.2 Energy spectroscopy

1. For the energy spectroscopy, the sources in the plastic case with an activity lower than 48 kBq are used. The sources can stay in the plastic case for the measurement.
2. In order to record the spectra, it is important to calibrate the electronics (amplifier etc.) as well as the multi-channel analyser so that the pulses are not over-amplified. Subsequently adjust the settings of the MCA amplifier so that the complete range of the analog-to-digital converter is used.
3. Write down the settings
4. Use the MCA to record the pulse height spectrum of all calibration sources. Take a measurement without source to estimate the background noise. The data can be saved as *.TKA files and copied to a USB flash drive.
5. Determine and write down the geometrical data.

Note : Bring a flash drive!

3.3 Compton scattering

For the measurement of Compton scattering, the two ^{137}Cs sources with activities > 20 MBq are used. Touch the sources only with pliers and hold them away from your body. Do not get to close to the sources and remove them before changing the setup.

1. Determine and minute the geometrical data.
2. Measurement of the differential scattering cross-section in ring geometry: Choose appropriate lead absorbers and scattering bodies and measure the Compton scattering for five angles between 10° and 50°. A measurement at 50° is required for comparison with the measurement at the same angle using the conventional geometry. Take care to create an axially symmetric setup.

   To estimate the background, record a measurement without the scattering body. This allows you to subtract the background rate later on.
3. Measurement of the differential scattering cross-section in conventional geometry: Again, perform measurements for five angles. Lead wedges for measurement angles of $50°, 65°, 80°, 95°, 105°$ and 135° are available. Take care to remove unwanted scattering volumes from the setup environment and make sure that the desired geometry is realised as exactly as possible. Perform this task with the scattering body made out of aluminium and the one made out of stainless steel. The measurement of count rates and background rate is performed as described in item 2.

4 Analysis

4.1 Energy spectroscopy

1. Interpret the recorded energy spectra.
2. Determine a calibration curve by plotting the photon energy as a function of the MCA channel number. Check if the curve is linear. If there are deviations, discuss them.
3. Measure the energy resolution of the scintillator for different energies by determining the widths of the photo peaks. Present them graphically. In a second figure, present the data in an appropriate way that allows determining the coefficients a and b from eq. (1).
4. Determine the detection efficiency ε. Use the measured rates in the photo peaks and present them graphically as functions of E_γ. Take into account the photon yield I_γ and the source activity $A(t)$ on the day of the experiment. Is there a linear relationship?
5. Use the ^{22}Na spectrum to determine the electron mass. Why is this source especially suited to this purpose?

4.2 Compton scattering

1. Discuss the data recorded at the same angle in conventional and ring geometry.
2. Determine the energy of the Compton scattered photons. Plot it as a function of the scattering angle. Compare your results with the theoretical expectation.
3. Determine the differential scattering cross-section for different scattering angles. Present your results graphically and discuss any deviations from the expected curve.

   Hint: The absorption η is the product of the absorption in air and aluminium / stainless steel and may be calculated from the attenuation coefficient μ. Measure the distance x_{Air} and x'_{Air} in front of and behind the scattering volume, respectively. Estimate the distances x_{Al} and x'_{Al}. Estimate, that the attenuation coefficient depends on material and photon energy.

   $$\eta = \exp\left(-\mu_{\mathrm{Air}}(E_\gamma)\cdot x_{\mathrm{Air}}\right)\cdot\exp\left(-\mu_{\mathrm{Al}}(E_\gamma)\cdot x_{\mathrm{Al}}\right)\cdot\exp\left(-\mu_{\mathrm{Al}}(E'_\gamma)\cdot x'_{\mathrm{Al}}\right)\cdot\exp\left(-\mu_{\mathrm{Air}}(E'_\gamma)\cdot x'_{\mathrm{Air}}\right)$$

   Values for μ may be found at [5].
4. For the angles covered by the conventional geometry, determine the scattering cross-section obtained using the stainless steel scatterer and compare the findings with the measurements using the aluminium. For the stainless steel scatterer, the properties of Iron may be used where required.
5. Plot $1/E'_\gamma - 1/E_\gamma$ as a function of $(1-\cos\theta)$. Determine the electron mass m_{e} from the line slope. Compare your result to that obtained in section 4.1, item 5.

Information about the activity and age of the radio-active sources are posted in the experiment room. **Perform a detailed analysis of uncertainties for all results!**

All decay schemes come from [**?**].

A ^{60}Co decay scheme

60CO B- DECAY (5.2714 Y)

Parent state: G.S.
Half life: 5.2714 Y(5)
Q(gs): 2823.64(11) keV
Branch ratio: 1.0

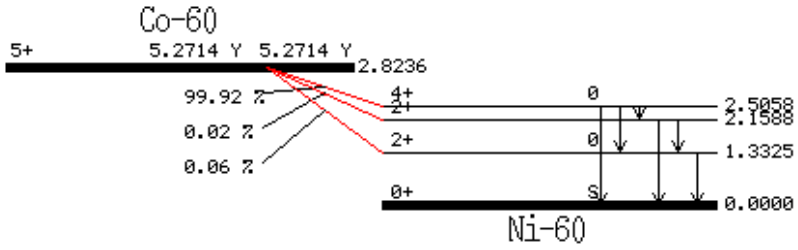

Beta ray:

Max.E(keV)	Avg.E(keV)	Intensity(rel)	Spin
1492(20)	625.87(5)	0.057(20)	5+
670(20)	274.93(5)	0.022(LT)	2+
317.88(10)	95.77(4)	99.925(20)	2+
			4+

Gamma ray:

Energy(keV)	Intensity(rel)
346.93(7)	0.0076(5)
826.28(9)	0.0076(8)
1173.237(4)	99.9736(7)
1332.501(5)	99.9856(4)
2158.77(9)	0.00111(18)
2505	2.0E-6(4)

M. M. KING, *Nuclear Data Sheet* 69,1 (1993)

60CO B- DECAY (10.467 M)

Parent state: 58.603(7) keV
Half life: 10.467 M(6)
Q(gs): 2823.64(11) keV
Branch ratio: 0.0024(3)

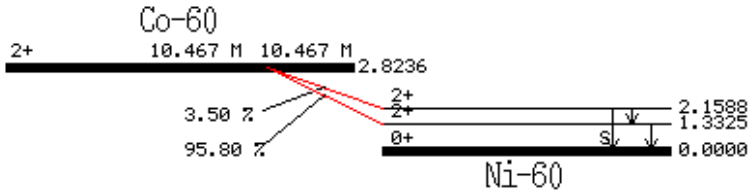

Beta ray:

Max.E(keV)	Avg.E(keV)	Intensity(rel)	Spin
1549.7(-)	606.37(5)	95.8(17)	2+
723.4(-)	248.80(6)	3.5(3)	2+
			2+

Gamma ray:

Energy(keV)	Intensity(rel)
826.28(9)	3.2(AP)
1332.501(5)	100
2158.77(9)	0.3(AP)

M. M. KING, *Nuclear Data Sheet* 69,1 (1993)

Please e-mail to *jhchang@kaeri.re.kr* for any comment. Thank you.

60CO IT DECAY

Parent state: 58.603(7) keV
Half life: 10.467 M(6)
Q(gs): () keV
Branch ratio: 0.9976(3)

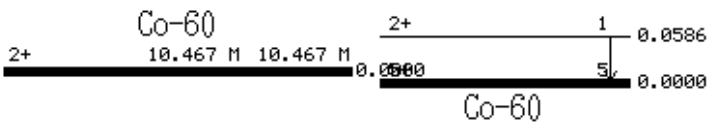

Gamma ray:

Energy(keV)	Intensity(rel)
58.603(7)	-

M. M. KING, *Nuclear Data Sheet* 69,1 (1993)

Please e-mail to *jhchang@kaeri.re.kr* for any comment. Thank you.

B ^{137}Cs decay scheme

137CS B- DECAY

Parent state: G.S.
Half life: 30.04 Y(3)
Q(gs): 1175.63(17) keV
Branch ratio: 1.0

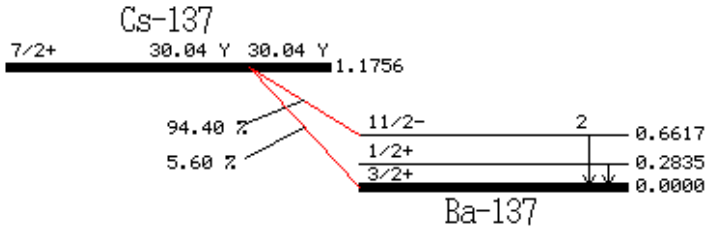

Beta ray:

Max.E(keV)	Avg.E(keV)	Intensity(rel)	Spin
7/2+			
1176(1)	416.264(72)	5.6(2)	3/2+
892.1(-)	300.570(68)	5.8E-4(8)	1/2+
514.03(23)	174.320(61)	94.4(2)	11/2-

Gamma ray:

Energy(keV)	Intensity(rel)
283.5(1)	5.8E-4(8)
661.657(3)	85.1(2)

J. K. TULI, *Nuclear Data Sheet* 81, 579 (1997)

Please e-mail to *jhchang@kaeri.re.kr* for any comment. Thank you.

C ^{152}Eu decay scheme

152EU B- DECAY (13.537 Y)

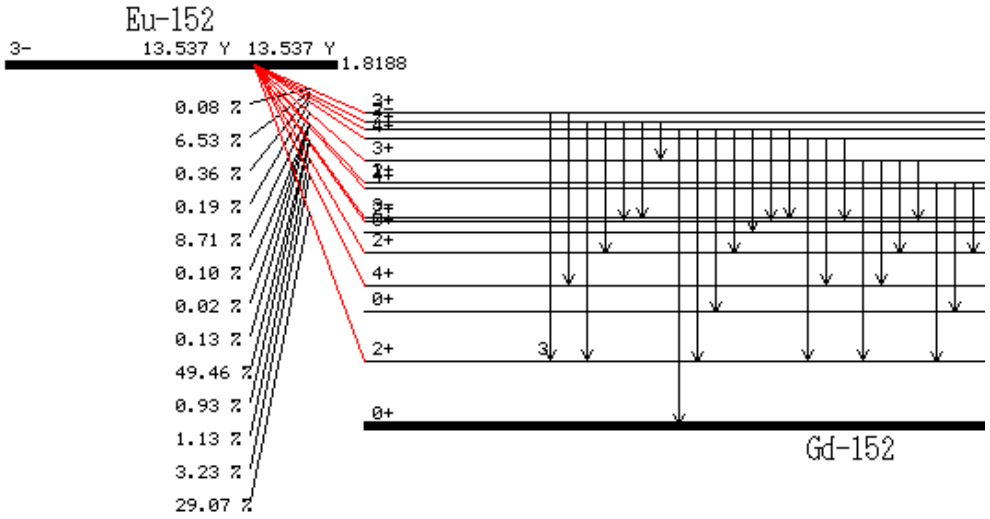

Parent state: G.S.
Half life: 13.537 Y(6)
Q(gs): 1818.8(11) keV
Branch ratio: 0.2786(30)

Beta ray: for absolute intensity multiply by 3.589

Max.E(keV)	Avg.E(keV)	Intensity(rel)	Spin
1474.5(-)	535.4(5)	8.1(5)	2+
1063.4(-)	364.6(5)	0.900(11)	4+
888.3(-)	295.1(5)	0.315(13)	2+
709.6(-)	226.9(5)	0.26(3)	2+
695.6(-)	221.7(4)	13.780(21)	3-
536.5(-)	164.1(4)	0.035(4)	4+
504.1(-)	152.7(4)	0.0050(11)	1-
500.4(-)	151.4(4)	0.0282(19)	2+
384.8(-)	112.3(4)	2.427(13)	3+
268.6(-)	75.2(4)	0.054(3)	4+
213.2(-)	58.5(4)	0.101(3)	2+
175.4(-)	47.4(4)	1.819(13)	2-
126.4(-)	33.4(3)	0.0213(19)	3+

Gamma ray: for absolute intensity multiply by 0.9519(11)

Energy(keV)	Intensity(rel)
173.17(15)	0.03(1)
192.60(4)	0.0256(8)
195.05(24)	0.023(5)
209.41(13)	0.0206(18)
271.131(8)	0.275(8)
315.174(17)	0.191(5)
324.83(3)	0.272(13)
344.2785(12)	100.0(16)
351.66(4)	0.035(5)
367.7887(16)	3.245(18)
387.90(8)	0.0110(8)
411.1163(11)	8.424(16)
440.86(10)	0.050(6)
482.31(3)	0.0053(23)
493.508(20)	0.037(4)
496.39(3)	0.0160(16)
503.474(5)	0.56(3)
520.227(5)	0.196(15)
526.881(20)	0.0495(24)
534.245(7)	0.161(4)
557.91(17)	0.017(7)
586.2648(25)	1.732(20)

615.4(1)	-
674.675(3)	0.064(6)
678.623(5)	1.777(16)
703.25(6)	0.006(2)
703.25(6)	0.013(3)
712.843(6)	0.35(3)
764.900(9)	0.81(9)
778.9040(18)	48.80(7)
794.81(3)	0.099(8)
930.580(15)	0.275(7)
937.05(15)	0.013(5)
974.09(4)	0.053(3)
990.19(3)	0.118(5)
1089.737(5)	6.513(24)
1109.174(12)	0.70(3)
1206.11(15)	0.053(4)
1261.343(23)	0.126(5)
1299.140(9)	6.12(3)
1314.7(2)	0.019(4)
1348.10(7)	0.067(4)
1605.61(7)	0.0308(18)

AGDA ARTNA-COHEN, *Nuclear Data Sheet* 79, 1 (1996)

152EU B- DECAY (9.3116 H)

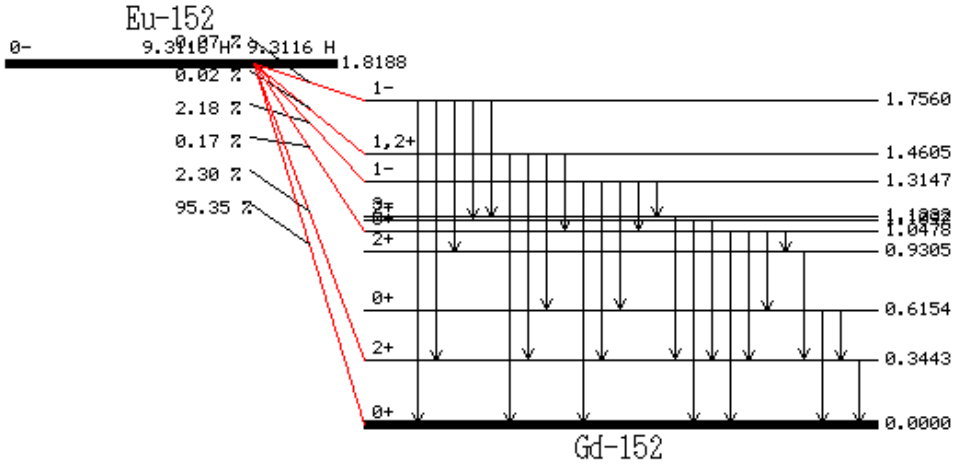

Parent state: 45.5998(4) keV
Half life: 9.3116 H(16)
Q(gs): 1818.8(11) keV
Branch ratio: 0.73(3)

Beta ray: for absolute intensity multiply by 1.37

Max.E(keV)	Avg.E(keV)	Intensity(rel)	Spin
1864.4(-)	704.0(5)	69.6(7)	0-
1520.1(-)	554.0(5)	1.68(25)	0+
816.5(-)	267.3(5)	0.123(18)	2+
549.7(-)	168.7(4)	1.59(24)	0+
403.9(-)	118.6(4)	0.0122(24)	1-
108.4(-)	28.4(4)	0.049(7)	1,2+

Gamma ray: for absolute intensity multiply by 0.195(29)

Energy(keV)	Intensity(rel)
117.3(3)	0.118(12)
191.6(3)	0.005(3)
266.91(22)	0.008(4)
271.06(1)	0.52(2)
344.31(3)	16.7(2)
412.0(3)	0.005(3)

432.52(10)	-
586.265(3)	0.089(6)
615.44(20)	-
632.8(3)	0.008(5)
646.9(3)	0.005(3)
699.27(4)	0.491(15)
703.54(5)	0.463(16)
764.900	0.003(2)
778.9045	0.013(6)
825.5(3)	0.005(3)
845.4(5)	0.063(9)
970.350(9)	4.13(14)
1048.1(3)	-
1109.174	0.002(1)
1116.0(10)	0.007(4)
1314.67(1)	6.54(10)
1411.70(3)	0.309(5)
1460.64(13)	0.011(3)
1755.94(6)	0.018(1)

AGDA ARTNA-COHEN, *Nuclear Data Sheet* 79, 1 (1996)

Please e-mail to *jhchang@kaeri.re.kr* for any comment. Thank you.

152EU EC DECAY (13.537 Y)

Parent state: G.S.
Half life: 13.537 Y(6)
Q(gs): 1874.3(7) keV
Branch ratio: 0.7188(5)

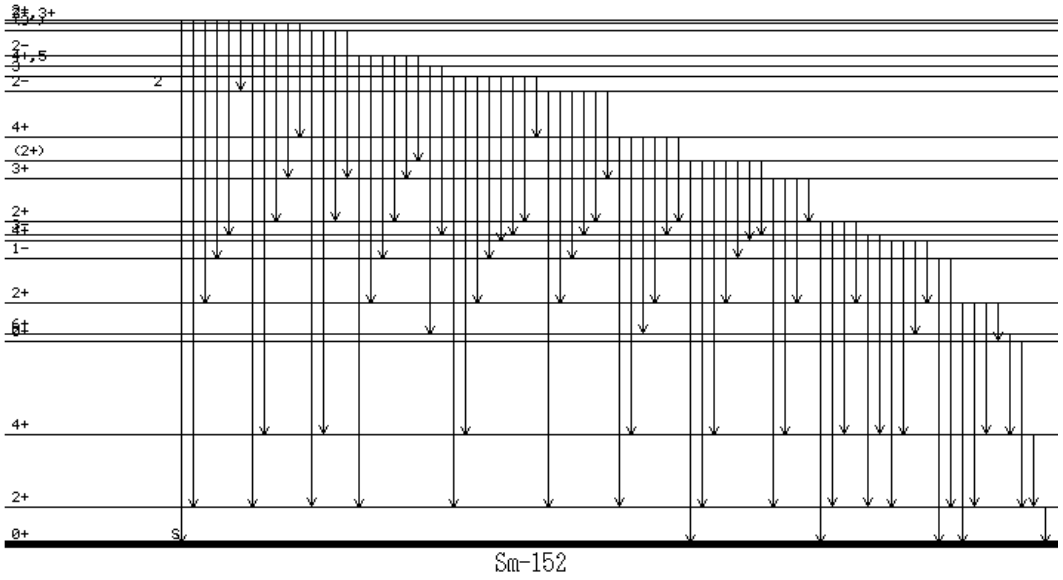

Beta+ ray: total intensity =1.92e-02
for absolute intensity multiply by 1.3912

Max.E(keV)	Avg.E(keV)	Intensity(rel)	Spin
730.5(-)	338.1(3)	0.011(2)	3- 2+
485.8(-)	230.7(3)	0.0028(7)	4+

EC: total intensity = 100.2

Gamma ray: for absolute intensity multiply by 0.3724(8)

Energy(keV)	Intensity(rel)
121.7817(3)	106.77(21)
125.69(13)	0.06(2)
148.010(17)	0.139(15)
175.18	0.015(4)
202.74(13)	0.019(4)
207.6(3)	0.0219(25)
209.10	-
212.568(15)	0.0741(20)
237.31(5)	0.035(5)
239.42(17)	0.017(7)
244.6975(8)	28.33(7)
251.630(7)	0.268(10)
269.86(6)	0.031(3)
275.449(15)	0.125(8)
285.98(3)	0.037(3)
295.9392(17)	1.669(19)
316.2(2)	0.008(5)
320.03(15)	0.006(2)
329.425(21)	0.48(3)
330.54(10)	0.022(6)
340.40(14)	0.136(10)
357.26(5)	0.015(3)
358.13	-
379.37(6)	0.0031(8)
385.69(20)	0.019(3)
387.90(8)	0.0110(8)
389.07(11)	0.013(5)
391.32(14)	0.0047(8)
395.75(19)	0.03(1)
406.74(15)	0.0031(8)
416.048(8)	0.411(7)
423.45(4)	0.0120(23)
440.86(10)	0.050(6)
441.00	-
443.965(3)	1.22(7)
443.965(3)	10.54(7)

482.31(3)	0.109(9)
482.43	-
488.6792(20)	1.565(12)
493.508(20)	0.110(8)
496.39(3)	0.019(3)
523.13(5)	0.056(6)
536.23	-
538.29(6)	0.0144(22)
556.56(3)	0.069(5)
561.2(5)	0.0039(8)
562.93(2)	0.010(5)
563.990(7)	1.828(23)
566.439(5)	0.482(7)
571.83(8)	0.018(3)
595.61(12)	0.12(4)
616.05(3)	0.034(3)
644.37(5)	0.023(3)
656.487(5)	0.541(7)
664.78(5)	0.062(9)
671.155(17)	0.073(6)
674.675(3)	0.644(16)
683.32(11)	0.012(3)
686.61(5)	0.072(6)
688.670(5)	3.20(3)
696.87(19)	0.06(3)
702.96	-
719.349(4)	1.04(3)
719.349(4)	0.22(3)
727.99(14)	0.042(3)
735.40(10)	0.022(4)
756.12(9)	-
768.944(9)	0.350(15)
805.70(7)	0.046(4)
810.451(5)	1.194(10)
839.36(4)	0.060(4)
841.570(5)	0.620(9)
867.373(3)	15.86(7)
896.58(9)	0.250(8)
901.181(11)	0.321(15)
906.01(6)	0.061(6)
919.330(3)	1.594(22)
926.317(15)	1.037(18)
958.63(5)	0.081(9)
963.390(12)	0.504(12)
964.079(18)	54.56(8)
968.00	0.014(9)
1001.1(3)	0.017(3)
1005.272(17)	2.412(17)
1084(1)	0.92(3)
1085.869(24)	38.13(8)
1112.069(3)	50.97(8)
1139(1)	0.0047(3)
1170.93(11)	0.138(10)
1212.948(11)	5.312(24)
1249.938(13)	0.703(14)
1292.778(19)	0.393(20)
1315.31(23)	0.027(6)
1363.77(5)	0.096(4)
1390.36(16)	0.018(3)
1408.006(3)	78.47(9)
1457.643(11)	1.875(17)
1485.9(3)	0.021(9)
1528.103(18)	1.051(17)
1608.36(8)	0.0198(14)
1635.2(5)	0.0006(2)
1647.41(14)	0.0236(21)
1674.30(6)	0.023(3)
1698.1(4)	0.022(7)
1769.09(5)	0.0357(14)

AGDA ARTNA-COHEN, *Nuclear Data Sheet* 79, 1 (1996)

152EU EC DECAY (9.3116 H)

Parent state: 45.5998(4) keV
Half life: 9.3116 H(3)
Q(gs): 1874.3(7) keV
Branch ratio: 0.27(3)

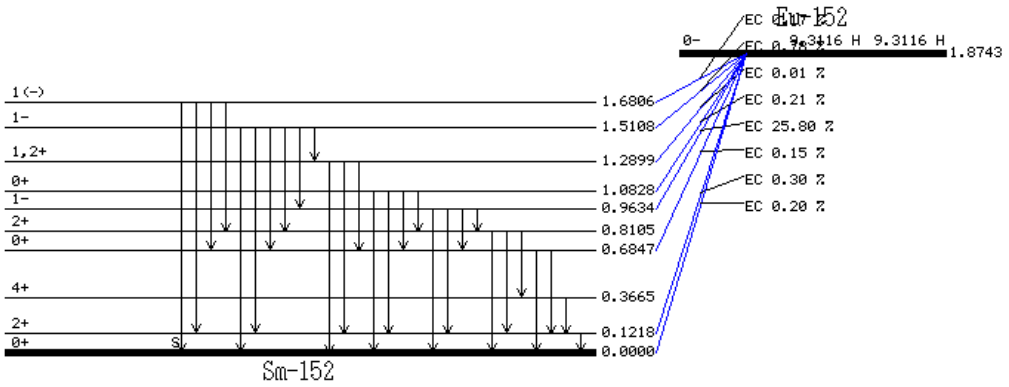

Beta+ ray: total intensity =2.74e-02
for absolute intensity multiply by 3.70

Max.E(keV)	Avg.E(keV)	Intensity(rel)	Spin	0-
897.9(-)	411.5(3)	0.0064(8)		0+
776.1(-)	376.4(3)	0.001(LT)		2+

EC: total intensity = 102.2

Gamma ray: for absolute intensity multiply by 0.525(10)

Energy(keV)	Intensity(rel)
121.777(5)	49.4(15)
152.9(3)	0.010(3)
160.0(5)	0.005(3)
218.1(3)	0.0003(2)
220.8(3)	0.0009(9)
244.70(1)	0.175(4)
256.99(22)	0.007(3)
272.41(4)	0.071(7)
278.7(3)	-
340.1(3)	0.035(13)
387.8(3)	0.005(3)
398.00(15)	-
443.96(4)	0.174(8)
547.35(8)	0.065(8)
562.93(2)	1.55(2)
605.0(5)	0.028(11)
684.85(20)	-
688.69(5)	0.458(14)
700.3(3)	0.075(13)
703.7(3)	0.005(3)
796.1(3)	0.024(10)
810.47(8)	0.176(8)
826.01(7)	0.005(3)
841.594(8)	100(2)
870.13(5)	0.621(13)
915.7(4)	0.07(1)
961.06(22)	1.40(7)
963.390(12)	82.3(7)
995.87(1)	0.48(1)
1039.2(5)	0.057(12)
1082.8(5)	-
1137.5(3)	0.09(6)
1168.16(19)	0.042(10)
1207.3(6)	0.020(7)
1290.0(5)	0.0063(6)
1389.00(1)	5.28(16)
1406.5(5)	0.005(3)
1420(1)	0.004(3)
1510.83(5)	0.045(3)
1558.73(3)	0.055(3)
1680.52(5)	0.037(2)

AGDA ARTNA-COHEN, *Nuclear Data Sheet* 79, 1 (1996)

Please e-mail to *jhchang@kaeri.re.kr* for any comment. Thank you.

152EU IT DECAY (96 M)

Parent state: 147.81(11) keV
Half life: 96 M(1)
Q(gs): () keV
Branch ratio: 1.0

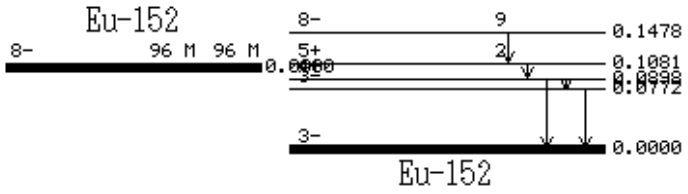

Gamma ray: for absolute intensity multiply by 0.699(6)

Energy(keV)	Intensity(rel)
12.598(15)	0.41(4)
18.21(4)	1.8(3)
39.75(10)	-
77.23(4)	0.98(7)
89.847(6)	100

AGDA ARTNA-COHEN, *Nuclear Data Sheet* 79, 1 (1996)

Please e-mail to *jhchang@kaeri.re.kr* for any comment. Thank you.

D ^{22}Na decay scheme

22NA B+ DECAY

Parent state: G.S.
Half life: 2.6088 Y(14)
Q(gs): 2842.0(5) keV
Branch ratio: 1.0

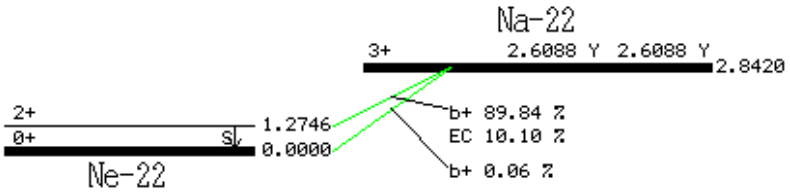

Beta+ ray: total intensity =89.9

Max.E(keV)	Avg.E(keV)	Intensity(rel)	Spin
1820.0(-)	835.00(23)	0.056(14)	3+
545.4(-)	215.54(21)	89.84(10)	0+
			2+

EC: total intensity = 10.1

Gamma ray:

Energy(keV)	Intensity(rel)
1274.53(2)	99.944(14)

P. M. ENDT, *Nuclear Physics* A521,1 (1990)

Please e-mail to *jhchang@kaeri.re.kr* for any comment. Thank you.